Plasmonics (2009) 4:79–93
DOI 10.1007/s11468-009-9078-2

Preparation of Gold Nanoparticles and their Applications in Anisotropic Nanoparticle Synthesis and Bioimaging

Ken-Tye Yong · Mark T. Swihart · Hong Ding · Paras N. Prasad

Received: 12 May 2008 / Accepted: 17 February 2009 / Published online: 28 February 2009

Abstract In this review, we highlight our recent achievements in using colloidal gold nanoparticles as building blocks for fabrication of anisotropic and multicomponent nanoparticles (e.g., nanoshells, semiconductor nanocrystals, and gold nanorods). The tunable optical properties of these nanoparticles are well suited for various biomedical and biophotonic applications.

Keywords Gold nanopaticle · Semiconductor nanocrystal · Nanorod · Bioimaging · Nanoshell · Seeded growth · Anisotropic nanocrystal

Introduction

Colloidal nanoparticle synthesis chemistry has experienced a renaissance in the last 10 years, driven by substantial improvements in the methods used to fabricate monodisperse nanosized colloidal particles [1, 2]. Scientists have found that when the size of these colloidal particles is sufficiently small, their properties can differ from those of the bulk materials, which makes them very attractive in applications ranging from physics to biology [1, 3, 4]. The development of these nanoparticles (NPs) has become a significant subject of chemical research, and they have led to advances in several areas of science and technology. A good example of the synergism between scientific discovery and technological development is the biomedical field, where discoveries of new luminescent semiconductor particles led to development of new optical probes for cancer and disease diagnosis, which had traditionally relied upon on organic dyes [5–13]. The progression of this nanotechnology will require the development of smaller, ultrasensitive, and smart multifunctional NPs, resulting in biomedical probes with different imaging modalities that allow noninvasive imaging for early detection of disease onset or real-time monitoring of disease treatment courses. For example, Nie's group has reported the use of multifunctional nanoparticle probes based on semiconductor quantum dots (QDs) for cancer targeting and imaging in living animals [14]. Their results strongly suggest that these unique functionalized particles are potential bioprobes for ultrasensitive and multiplexed imaging of molecular targets in vivo. Bawendi's group demonstrated that quantum dots allow a major cancer surgery, sentinel lymph node mapping, to be performed in large animals under complete image guidance [15]. More recently, they defined the requirements for renal filtration and urinary excretion of quantum dots [16]. Prasad's group demonstrated the use of InP/ZnS QDs as non-cadmium-based highly biocompatible QDs for two photon imaging of cancer cells [17]. Halas' group has demonstrated a gold nanoshell-based all-optical platform technology for cancer imaging and therapy applications [18–20]. More specifically, they have engineered the nanoshells to scatter light in the near-infrared (NIR), which enables optical cancer imaging, and to absorb light, which allows selective destruction of targeted carcinoma cells through photothermal therapy. El-Sayed's group has demonstrated the application of gold NPs and nanorods (NRs) as novel contrast agents for both in vitro

K.-T. Yong · M. T. Swihart (✉) · H. Ding · P. N. Prasad
Institute for Lasers, Photonics and Biophotonics,
State University of New York at Buffalo,
Buffalo, NY 14260–4200, USA
e-mail: swihart@eng.buffalo.edu

M. T. Swihart
Department of Chemical and Biological Engineering,
State University of New York at Buffalo,
Buffalo, NY 14260–4200, USA

molecular imaging and photothermal cancer therapy [21, 22]. All these fascinating findings suggest that NPs will play an important role in the future health care and disease treatment.

Scientists are increasingly capable of manipulating the shape and composition of colloidal particles, which in turn affects their unique optoelectronic properties [23–28]. These non-spherical particles are ideal candidates for biomedical applications such as biosensors and contrast agents for diagnosis of human diseases. For example, our group has shown the application of carefully designed quantum rods (QRs) in confocal and two-photon imaging of cancer cells (see Fig. 1) [29, 30]. Also, we have used QRs for in vivo imaging studies (see Fig. 2). Alivisatos' group has reported that quantum rods were brighter single molecule probes than quantum dots [31]. Chao et al. [32] have presented the detection of prostate-specific antigen with n-type In_2O_3 nanowires (NWs) and p-type carbon nanotubes. Gao et al. [33] have demonstrated the use of a silicon NW array for direct electrical detection of DNA at femtomolar levels. Shi Kam et al. [34] created functionalized single-wall carbon nanotubes (SWNTs) with a folate moiety for selective cancer cell destruction without harming the normal cells. These encouraging results on anisotropic nanomaterials as biological markers and sensors may provide an avenue for further improvements in ultrasensitive imaging and detection strategies.

This review is focused on the latest advances in our group on solution phase synthesis of anisotropic and hybrid nanomaterials. We describe the use of gold NPs to produce metallic nanoshells, anisotropic semiconductor nanocrystals (NCs), and gold NRs, as well as the properties and some biophotonics applications of these nanomaterials. These particles are very interesting from the point of view of their optical properties, which strongly depend on the particle size, shape, composition, and surface coating. The basic methods of synthesizing gold NPs are first described in "Synthesis of gold NPs" since their sizes directly affect the final shape or structure of the seeded or functionalized particles. "Nanoshell fabrication using gold NPs" describes our results on fabrication of gold and silver nanoshells using gold NPs and the influence of the initial size of the gold NPs on the nanoshell morphology and properties. "Anisotropic growth of semiconductor nanocrystals using gold NPs" focuses on using gold NPs to promote anisotropic growth of semiconductor nanocrystals. "Synthesis of gold NRs" summarizes our strategy of using various suitable additives (e.g., co-surfactants and electrolytes) to tailor the morphology ofgold NRs, and finally, "Application of gold NRs in bioimaging" briefly describes some bioimaging applications of these functionalized nanomaterials.

Synthesis of gold NPs

Gold NPs have been a subject of intensive research for the last 20 years due to their interesting optical and catalytic properties [35]. Michael Faraday was the first to scientifically investigate their synthesis and unique optical properties [36]. In 1857, he prepared stable gold colloids by reducing gold chloride with phosphorus in water. To date, his original samples are still preserved and on display at the Faraday Museum in London. Even before the "actual" discovery by Michael Faraday, colloidal gold was commonly used to stain glass to provide a ruby-like color. For example, gold was used in the ruby colored glass window in Milan Cathedral, Italy, made by Niccolo da Varallo in ~1486, illustrating the birth of St. Eligius, patron saint of goldsmiths [37].

Gold NPs are well known for their surface plasmon resonance (SPR) properties, which originate from collective oscillation of their conduction electrons in response to

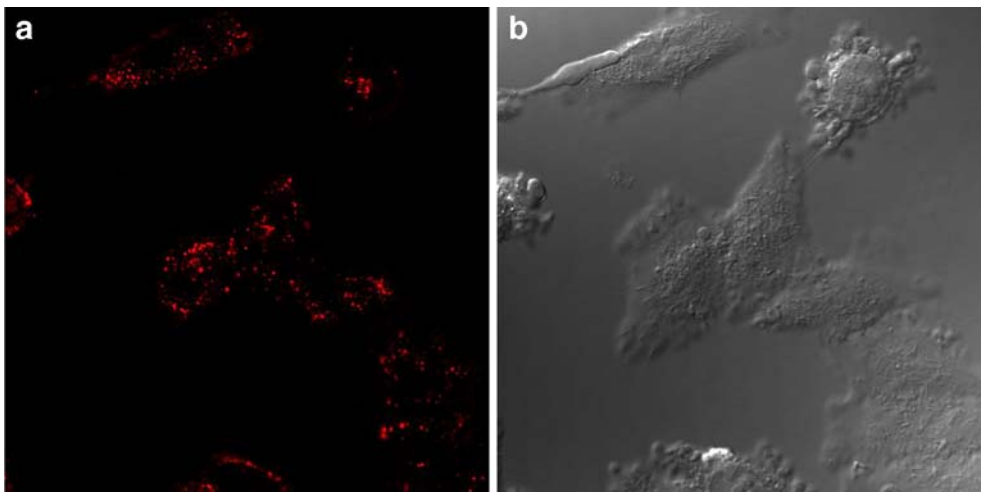

Fig. 1 Confocal microscopy images of HeLa cells labeled with transferrin-conjugated CdSe/CdS/ZnS quantum rods; **a** fluorescence image and **b** the corresponding transmission image

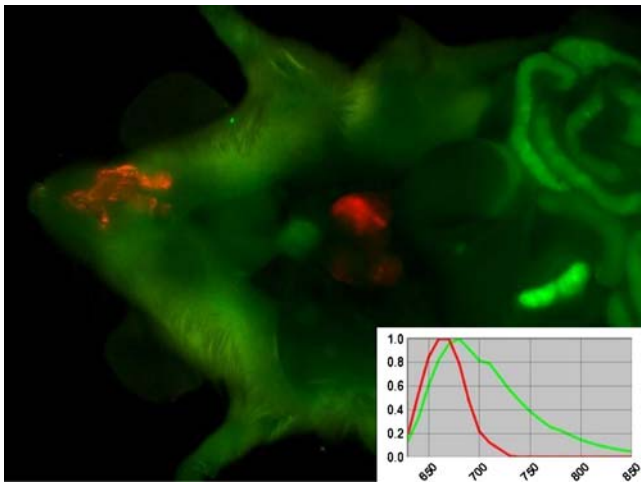

Fig. 2 In vivo fluorescence imaging of a mouse instilled with QRs by pharyngeal aspiration. This approach is used to investigate the biodistribution and toxicity of QRs on small animals. The image was acquired using Maestro™ FLEX In Vivo Imaging System. Tissue autofluorescence is shown in *green*, while the unmixed QR signal is shown in *red*. The corresponding fluorescence spectra of QR and autofluorescence are shown in the *inset*

optical excitation [38]. The SPR frequency of gold NPs has been shown to depend on particle size, shape, and dielectric properties, aggregate morphology, surface modification, and refractive index of the surrounding medium. For example, the SPR peak of 13 nm spherical gold colloids is around 520 nm and that of 5–6 nm silver NPs is around 400 nm. Gold NPs have been used in display devices, catalysis, biological markers, DNA sensors, surface-enhanced Raman scattering, and electronics [39–44]. The synthesis and characterization of gold NPs have thus attracted considerable attention from both fundamental and practical points of view. To date, many methods including chemical reduction of metal salts, photolysis or radiolysis of metal salts, ultrasonic reduction of metal salts, and displacement of ligands from organometallic compounds have been used to prepare gold NPs [36].

In situ chemical reduction of tetrachloroauric acid ($HAuCl_4$) precursor is perhaps the most popular route for synthesizing gold NPs. Reducing agents such as sodium or potassium borohydride [45], hydrazine [46], ascorbic acid [47], nitric/hydrochloric acid [45], and dimethyl formamide [48] are commonly used in the reduction of metal ions. When a reducing agent is added to the solution containing the metal salt, the metal ions are reduced and metallic solid particles are nucleated. Because NPs tend to be unstable in solution, special precautions have to be taken to avoid their aggregation or precipitation. The most common strategy is to employ surfactants as capping agents, which not only prevents aggregation but also results in functionalized and stabilized metal particles [49]. For example, cystine [50], ionic, and nonionic surfactants [51], CS_2 [52], sodium citrate [53], nitrilotriacetate [54,] 3-aminopropyltrimethoxysilane [55], 2-mercaptobenzimidazole [56], and dendrimers [57] have been used as surface active agents that bind to the gold NPs to both limit particle growth and to create a stable colloidal dispersion. Previous studies have also shown that the metal particles can be successfully synthesized without stabilizing agents. However, the colloidal stability of particles prepared with "bare" surfaces is usually temporary.

In our group, four kinds of gold NPs were prepared, with their sizes, surface coating, and surface charges specifically tailored for advanced fabrication of nanomaterials. The four types of gold NPs are, namely, citrate-capped gold NPs, tetrakis(hydroxymethyl)phosphonium chloride (THPC)-capped gold NPs, cetyltrimethylammonium bromide (CTAB)-capped gold NPs, and organically dispersible dodecylamine (DOD)-capped gold NPs. Both citrate-capped gold and THPC-gold particles are used to decorate the surface of PS spheres, where they were used as nucleation sites for synthesis of metallic nanoshells. CTAB-gold NPs are specifically used to obtain monodisperse gold NRs by a seed-mediated growth approach. Lastly, DOD-gold NPs are utilized as seeds to direct the one- and two-dimensional growth of semiconductor nanocrystals by hot colloidal synthesis. In the next few subsections, we briefly discuss the synthesis methods for each type of gold NPs as well as their physical and optical properties.

Citrate-capped gold NPs

Gold NP production by citrate reduction of $HAuCl_4$ in water was first introduced by Turkevitch in 1951 [58]. Since then, various modifications were made to the original recipe to obtain particles of different size. Particles produced by this approach are hereafter called citrate-gold. In brief, to make citrate-gold, $HAuCl_4$ solution is heated at 90 °C. Next, a freshly prepared sodium citrate solution is introduced to the hot solution. A few minutes later, the solution will change from colorless to a deep wine-red. The resulting red sol contains citrate-gold NPs approximately 12 nm in diameter and has a sharp SPR peak at 520 nm (see Figs. 3 and 4).

THPC-capped gold NPs

For the preparation of THPC-gold NPs, the method described by Pham et al. was adopted [59]. Basically, a freshly prepared mixture of NaOH and THPC solution is added to a flask containing pure HPLC water. The reaction mixture is aged and then $HAuCl_4$ solution is added. The color of the mixture slowly changes from yellow to dark brown, indicating the formation of THPC-gold NPs. The reduction of chloroauric acid with THPC results in relatively

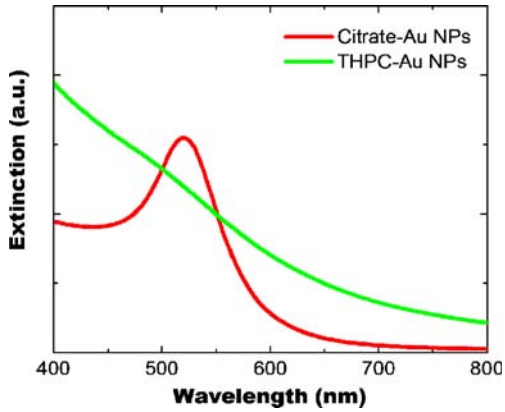

Fig. 3 Absorption spectra for citrate-gold and THPC-gold NPs

small gold NPs, ~2 nm in diameter, with a net negative interfacial charge. For THPC-gold NPs, no SPR peaks are observed, which is consistent with many literature reports that there is no SPR feature for such small Au particles (see Fig. 3).

CTAB-capped gold NPs

The synthesis of CTAB-gold NPs was first reported by Nikoobakht et al. [60]. The CTAB-gold NPs are frequently used as seeds for the synthesis of monodispersed gold NRs with various aspect ratios. The fabrication of CTAB-gold NPs is straightforward and simple. Briefly, CTAB solution is mixed with $HAuCl_4$ solution. Ice-cold $NaBH_4$ solution is quickly added, resulting in the formation of a light-brown solution. The average size of these gold seeds is ~4 nm, with a net positive interfacial charge [61]. For CTAB-gold NPs, similarly, no SPR peaks are observed.

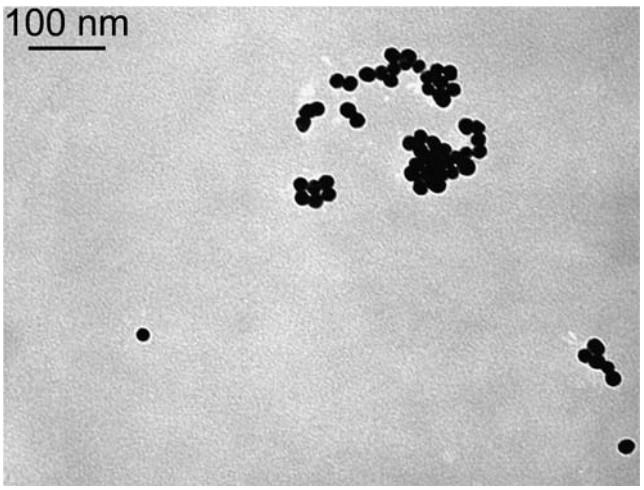

Fig. 4 TEM image of citrate-gold NPs. The particles size is estimated to be 12 nm

Organically dispersible dodecylamine passivated gold NPs (DOD-gold NPs)

Brust's two-phase method for gold NP synthesis was first published in 1994 and had a very strong impact on the nanoparticle field because it allowed the facile synthesis of thermally stable and air-stable gold NPs of reduced dispersity and controlled size for the first time (with diameter between 1.5 and 5.2 nm) [62]. In general, to synthesize these particles, a bright yellow $HAuCl_4$ solution is mixed with tetraoctylammonium bromide solution. The mixture is vigorously stirred. Phase separation occurs immediately, yielding an orange/red organic phase on top and a clear/slightly orange tinted aqueous phase on the bottom. The organic phase is separated, and the aqueous phase is discarded. Dropwise addition of $NaBH_4$ solution, with stirring, produces an instant color change of the organic phase, from an orange-red to a deep-red color. In general, these particles were readily dispersible in toluene, chloroform, and tetrahydrofuran and could be repeatedly precipitated and redissolved. By increasing the surfactant to precursor ratio, the SPR peak can be tuned from ~535 to ~500 nm, indicating that the particle size decreases as the dodecylamine surfactant concentration increases (see Fig. 5). Figure 6 shows a TEM image of the typical DOD-gold NPs synthesized using 0.12 g of dodecylamine.

Nanoshell fabrication using gold NPs

Nanoshells are spherical nanoparticles consisting of a dielectric core (e.g., silica or polystyrene) covered by a thin layer of metal. These structures have a tunable SPR that gives rise to intense optical absorption and scattering [63]. In this core-shell morphology, the plasmon resonance frequency of the nanoparticle can be tuned by changing the

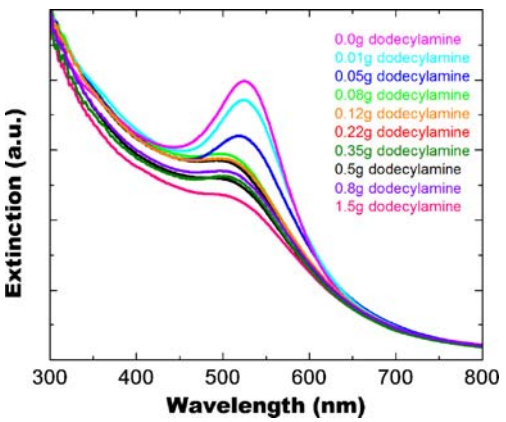

Fig. 5 Absorption spectra for different sizes of DOD-gold NPs; the gold NPs size decreases as the concentration of dodecylamine increases

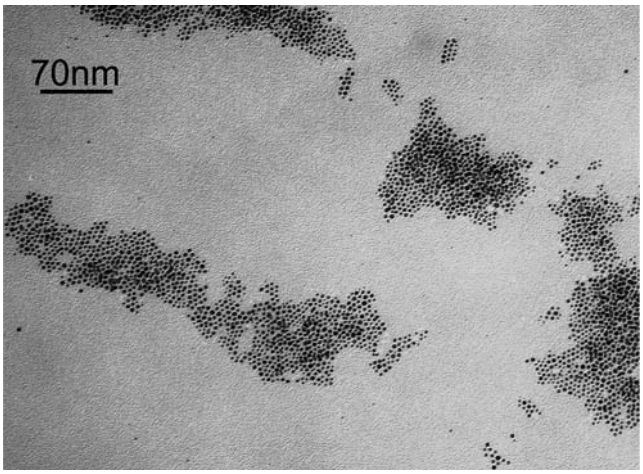

Fig. 6 TEM image of DOD-gold NPs

shell thickness relative to the diameter of the core. Nanoshells can be fabricated with optical resonances from the visible to the near-infrared region of the spectrum, easily spanning the key part of the spectrum (700–1,300 nm), where optical transmission through tissue is optimal. To date, the usefulness of metallic nanoshells has been demonstrated in applications ranging from photooxidation inhibition in photoluminescent polymer films, to Raman sensors that can be optimized to specific pump laser wavelengths, to optically triggered drug delivery [64]. Since gold nanoshells offer the added features of high biocompatibility and facile bioconjugation to antibodies via general protocols adapted from gold colloid bioconjugate chemistry, their near-infrared optical properties make them an ideal candidate for a whole blood immunoassay.

Recently, we have reported the fabrication of silver and gold nanoshells on polystyrene (PS) spheres of different diameters, ranging from 145 to 543 nm, using a solution phase synthesis technique [65, 66]. In our approach, the carboxylate-terminated polystyrene spheres were first functionalized with 2-aminoethanethiol hydrochloride to obtain thiol-terminated microspheres. Next, a partial layer of the citrate-gold NPs or THPC-gold NPs was attached onto the surface of thiol-terminated microspheres. These were further grown in the presence of excess metal ions (silver or gold) to render a complete shell. By varying the absolute shell thickness of the silver or gold on the polystyrene spheres, the peak of the surface plasmon absorbance band was tuned from the visible to the near-infrared (~500–940 nm; see Fig. 7). Representative TEM images of gold nanoshells with different shell coverage formed on 188 nm THPC-gold-decorated PS NPs are presented in Fig. 8. It was observed that the gold nanoshells fabricated using formaldehyde as reducing agent have a more uniform coating than those prepared using sodium borohydride or hydroxylamine hydrochloride. In general, it is very important that all small gold NPs grow evenly on the particle surfaces, so that after the gold particles have grown to a few nanometers, all particles will coalescence, and the resulting gold shell has a uniform thickness. Also, we observed that necklace-like chain aggregate structures of gold core-silver shell NPs could be formed by reducing silver nitrate directly onto free citrate-gold NPs. The plasmon resonance absorption of these aggregates could also be systematically tuned across the visible spectrum.

Anisotropic growth of semiconductor nanocrystals using gold NPs

A growing array of synthetic methods has been developed to produce nearly monodispersed spherical NCs [67–69]. Nanometer-sized particles of semiconducting materials allow control of the electronic and optical properties by control of the particle size [70]. Once the diameter of the nanoparticle becomes smaller than the bulk exciton radius, the energy levels in these nanometer sized particles become quantized, and the transitions are locked into discrete energy states, as opposed to the band structures in bulk semiconductors. Under these size limits, producing quantized (discrete) energy levels, the NCs are also called QDs. They can be synthesized in organic phase followed by surfactant exchange and additional surface functionalization as needed for subsequent applications or to be dispersed in aqueous systems. The use of semiconductor QDs as luminescence probes for numerous biological and biomedical applications has become an area of intense research focus over the last few years [71, 72]. These unique luminescent materials can have significant advantages over traditional fluorescent probes like organic dyes and fluorescent proteins. For example, QDs with different emission

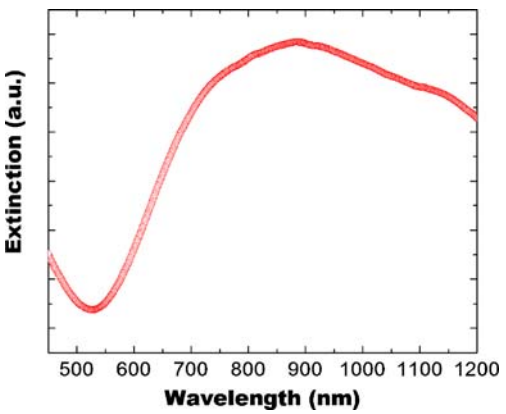

Fig. 7 Absorption spectra of gold nanoshells fabricated with a ~145-nm diameter polystyrene core and ~25-nm thick gold shell. The stable solution of gold nanoshells possesses a strong extinction peak at ~870 nm

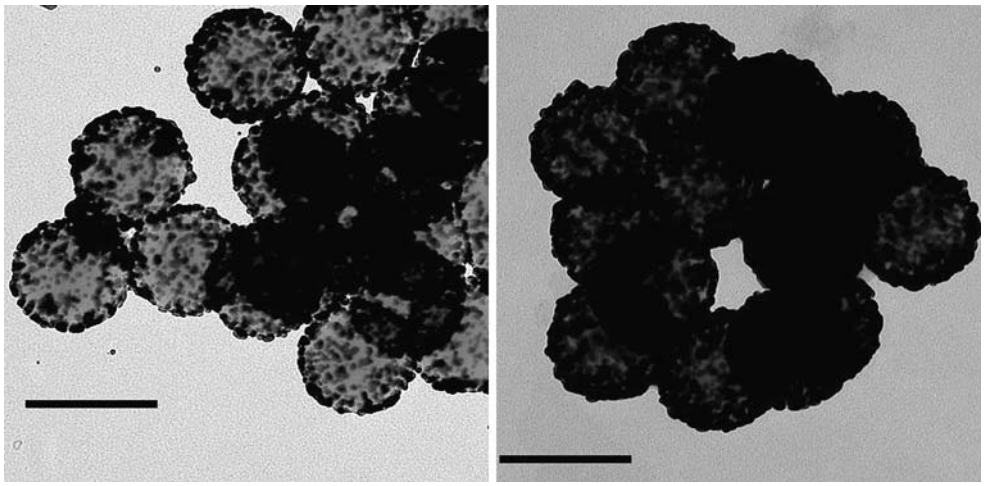

Fig. 8 TEM images of gold nanoshells with different coverage of gold shell; the *scale bar* is 200 nm

colors can be simultaneously excited with a single light source, with minimal spectral overlap, providing significant advantages for multiplexed detection of molecular targets. Also, QDs have been shown to remain brightly emissive even after long periods of excitation, whereas organic dyes are photobleached quickly. Furthermore, QDs can be tuned to emit in a range of wavelengths by changing the nanoparticle size, shape, and composition, whereas new organic dye moledcules must be designed to shift their emission towards desirable wavelengths. This flexibility in optical tuning allows the QDs to emit in the NIR region, which is optimal for imaging through tissue. Thus, the size-tunable emission from the visible to infrared wavelengths, broad absorption spectra, and superior brightness and photostabilty of QDs have led to their development as a new generation of optical probes for diagnostic imaging [73].

Interesting behavior is observed when semiconductor NC shape evolves from zero-dimensional (0D) QDs to one-dimensional (1D) quantum rods (QRs) or nanowires (NWs). For example, it was reported that CdSe QRs emitted light that was linearly polarized along the *c*-axis of the crystallites and that the degree of polarization was dependent on the aspect ratio of the NCs [23]. These early studies of anisotropic NCs show that nanostructures of different shapes (e.g., QRs and NWs) can offer new possibilities for tailoring material properties and offer improved performance when they are used as functional components in lasers or various other memory and optoelectronic devices [74–83]. To date, two major syntheses methods have been found to be very useful in tailoring the shape of semiconductor NPs. Gas-phase syntheses such as the vapor–liquid–solid (VLS) method and thermal evaporation are powerful tools to fabricate low-dimensional nanocrystals [84, 85]. For example, architectures including wires, tubes, ribbons, and other more complex shapes have been produced using the gas-phase approaches. On the other hand, the liquid phase synthesis approach usually provides more convenient, facile, and reproducible routes for producing nanocrystals with controllable sizes and shapes [86]. More importantly, this technique is scalable for higher production yield [87, 88]. This technique also enables the resulting NPs to be easily dispersed in organic or aqueous media for numerous potential applications where solution-phase processing such as ink-jet printing, spin-coating, and roll-to-roll coating is beneficial. Thus, the aim of our research is to provide general strategies to tailor the shape and size of semiconductor NCs. More importantly, we have identified underlying mechanisms of the anisotropic nanocrystal growth that will provide the colloidal synthesis scientific community with helpful guidelines for tailoring the shape of NPs for specific technological applications.

In general, the colloidal growth of nonspherical NCs is achieved by one of two methods [2]. In one approach, the reaction is carried out in the presence of a mixture containing at least two surfactants with significantly different affinities for different NC faces, such as a phosphonic acid and a long-chain carboxylic acid or amine [89, 90]. In hexagonal II–VI semiconductors, the strongly adsorbed phosphonic acid slows the growth of the nanocrystal and results in preferential growth along the *c*-axis of the wurtzite structure. In this method, a high precursor concentration is maintained, often via multiple injections of the precursors into the reaction pot during the growth of the nanocrystal. Another approach is the solution–liquid–solid (SLS) method, analogous to the (VLS) approach for growing NWs from vapor precursors [91]. This method uses metallic NPs as seeds to promote anisotropic crystal growth. The metallic seed particles melt, precursor atoms dissolve in them, and crystal growth occurs at the metal's liquefied surface. This provides a lower energy path to nucleation than homogeneous nucleation in the solution phase [92]. NC rods or wires of materials including InP, InAs, and Si have been prepared using metallic NPs as

seeds [93]. Growth of CdSe, CdTe, CdS, and PbSe wires by the SLS method using bismuth-coated gold NPs has been reported, although those experiments were carried out by technical grade (90%) trioctylphospine oxide containing phosphonic acids that may also promote anisotropic growth [94, 95].

Many excellent studies on the shape control of colloidal nanocrystals have been demonstrated. However, the ability to predict the final form of building blocks is still not fully understood. If a general synthesis scheme can be developed to control the shape of the nanocrystals, we could desirably program the reaction system to produce the final building blocks with desired shape, size, composition, and crystallinity. For the past 2 years, our group has done a series of systematic investigation on the shape control of II–VI and IV–VI nanocrystals by seeding their growth with gold NPs under conditions where the seed particle does not melt. CdSe, CdS, PbS, and PbSe nanocrystals with different morphologies such as cylinders (QRs), wires, plates, multipods, cubes, crosses, stars, and branched structures were produced. It was found that the most important parameter in determining the shape, size, and structure of NCs is the concentration of the metal NPs and the precursor ratio. In the next few sections, we will discuss the general synthesis approach that we have developed for fabricating anisotropic CdSe, CdS, PbS, and PbSe nanocrystals. The anisotropic growth mechanism of the nanocrystals will also be addressed.

Synthesis of anisotropic CdSe NPs

CdSe has a direct band gap of 1.89 eV and a Bohr radius of 4.9 nm [96]. It is commonly used in photovoltaics and in light-emitting diodes for flat-panel displays [1]. Various methods to tailor the shape and size of CdSe nanocrystals (NCs) have been reported [3]. For example, CdSe NWs have been fabricated by a solution process [97, 98] and high temperature evaporation [99]. CdSe quantum rods were prepared by solution techniques using structure-directing agents [23], micellar templating techniques [100], and microwave techniques [101].

To date, metal NPs have been used to induce one-dimensional nanocrystal growth in other systems including CdSe, CdS, CdTe, and PbSe with Bi/Au core/shell material [94, 97, 98, 102], InAs with Au, Ag, or In, and Si and Ge with Au [103–105]. In these cases, the growth is proposed to occur via the SLS mechanism [106], in which the metal NPs melt and serve as nucleation sites where a supersaturated precursor solution is converted into a crystalline product. Recently, we have developed a single pot colloidal synthesis approach for producing CdSe multipods and rods using DOD-gold NPs as seeds [107]. In the presence of these gold seeds, CdSe multipods and rods were obtained (see Fig. 9). It was found that most of the anisotropic growth took place during the first few minutes immediately after injection of the reaction precursors. The initial population of the multipods decreased and that of the rods increased significantly as the reaction time progressed. Also, we note that a gold particle is sometimes present at the center of the multipod structure (see Fig. 10) although homo-multipods constitute the dominant population. Details of the anisotropic growth mechanism will be addressed in "Comparison of anisotropic growth mechanism between the CdSe and PbSe system."

Synthesis of CdS nanoplatelets

CdS is one of the most important semiconductors in the II–VI group [108]. This well-studied semiconductor has a direct band gap near 2.4 eV (similar for both cubic and hexagonal polymorphs) at room temperature, and it is currently used for photoelectric conversion in solar cells, in light-emitting diodes for flat-panel displays and other optical devices [109, 110]. For the past several years, various synthesis methods have been developed to control the semiconductor nanocrystal morphology [111]. For example, thin CdS NWs were synthesized by laser ablation [112]. Solution-based routes with the presence of surfactants were used to synthesize one-dimensional CdS nanostructures, such as NRs, NWs, nanotubes, and nanobelts [113–115]. Our research focused mainly on applying gold NPs to control the shape of the CdS nanocrystals [116]. By simply adjusting the concentration of DOD-gold NPs and reaction temperature, CdS nanocrystals with platelet morphology were obtained. Figure 11 shows a TEM image of the nanocrystal product composed of triangular, rectangular, pentagonal, and hexagonal CdS nanoplatelets synthesized in the presence of gold NPs. These can form a two-dimensional

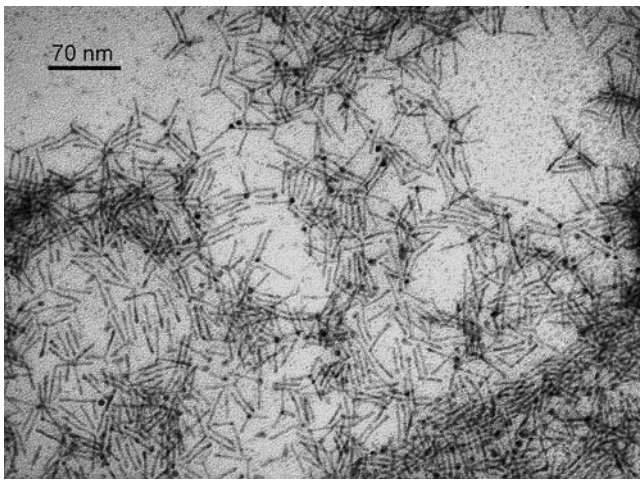

Fig. 9 TEM image of quantum rods and bipods synthesized using gold NPs

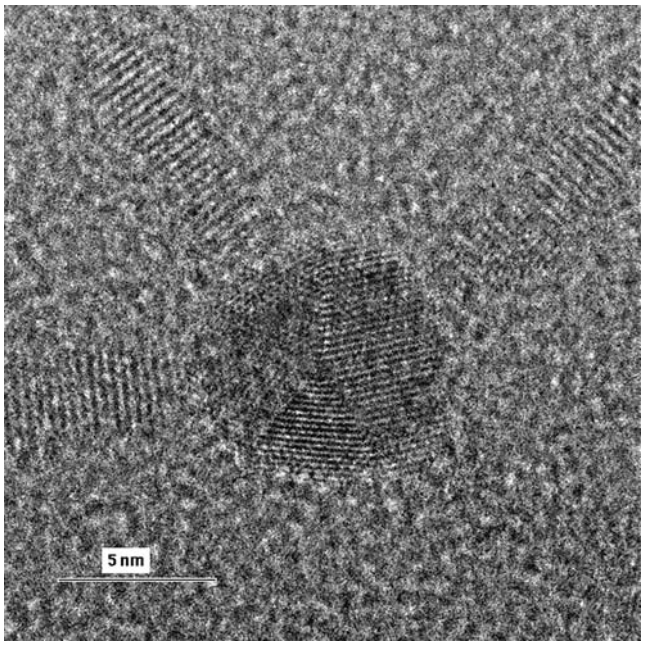

Fig. 10 HRTEM image of multiple CdSe quantum rods growing out from a single gold nanoparticle

nearly close-packed array. At present, the role of gold NPs in directing the growth of nanoplatelets is not fully understood, but it appears that they induce nucleation of the wurtzite phase under conditions where the zinc blend phase would preferentially nucleate in the absence of seed particles. Further detailed studies are needed to map out the mechanism of formation of CdS nanoplatelets in the presence of gold NPs.

Synthesis of anisotropic PbSe NPs

Lead chalcogenides (PbS, PbSe, and PbTe) are very promising materials for thermoelectric applications [117–119]. Especially, PbSe, an important binary semiconductor with small room temperature band gap (~0.28 eV) and large exciton Bohr radius (46 nm), has attracted great attention due to its wide potential applications in optical devices as optical switches, near-IR communication, thermal, and biologic images, and photovoltaic solar cells [120–122]. For example, our group has demonstrated the efficient photosensitization at ~1,550 nm of a polymeric nanocomposite with colloidally fabricated PbSe semiconductor quantum dots as the photoactive constituent [123]. We have demonstrated the fabrication of PbSe NCs in a variety of shapes using DOD-gold NPs as seeds [124]. The shape and size of the PbSe NCs strongly depend on the concentration of the metal particles and on the Pb to Se ratio in the growth solution. We have discovered that at low concentration of gold NPs (~0.0005 mmol metal atoms), QRs and T- and L-shaped particles were formed, with QRs constituting the vast majority of the population (>80%) as shown in Figs. 12 and 13. When the gold NP concentration was increased (≥0.025 mmol metal atoms), other morphologies such as cross-shaped PbSe NCs and gold core-PbSe shell structures were formed (see Fig. 14). In this case, we expect that the essential contribution of the seed particle is simply to provide a low energy interface for heterogeneous nucleation of the PbSe nanocrystal that promoted the anisotropic growth. Further discussion and comparison between the growth mechanism of PbSe and CdSe system will be made in "Comparison of anisotropic growth mechanism between the CdSe and PbSe system."

Synthesis of anisotropic PbS NPs

PbS is an attractive sulfide semiconductor with a band gap energy of 0.41 eV and large excition Bohr radius [125]. It has been used in applications mentioned above. Recently, an exceptional third-order nonlinear optical property of PbS

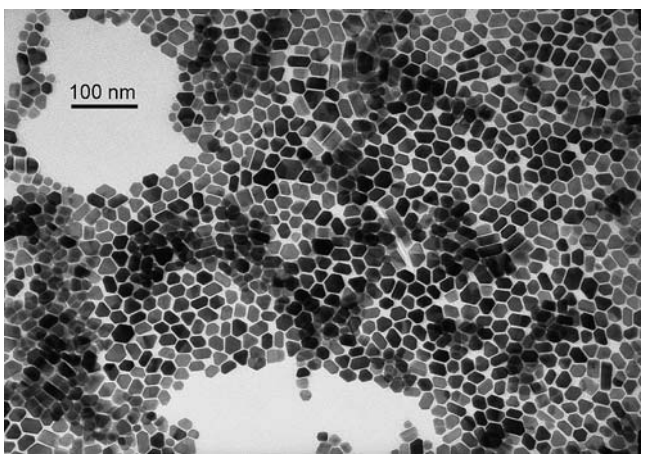

Fig. 11 TEM image of CdS nanoplatelets synthesized using gold NPs

Fig. 12 TEM image of PbSe quantum rods. More than 80% of the population is quantum rods

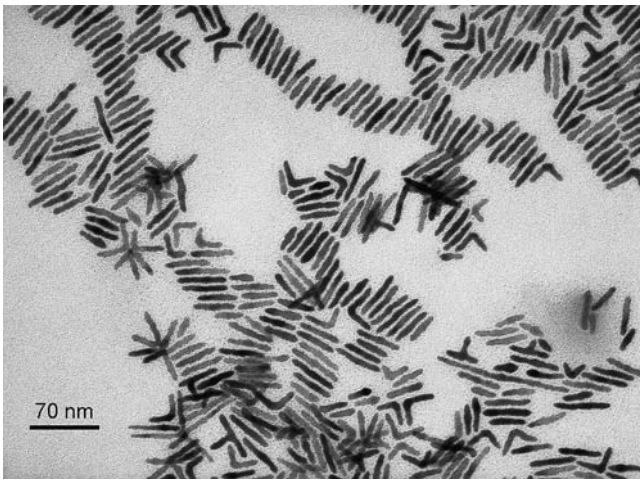

Fig. 13 TEM image of PbSe quantum rods with higher magnification

Fig. 15 TEM image of PbS NWs using gold NPs

NPs has been found, which may be useful in optical devices such as light-emitting diodes and high-speed optical switches [126, 127]. The synthesis of PbS particles with a variety of morphologies has been achieved by various methods [128]. For example, rod-like PbS nanocrystals have been produced using a combination of surfactant and polymer matrix as the template [129]. PbS NWs as well as nanosheets have been prepared by a polymer-assisted solvothermal method [130]. These results establish that it is possible to control the morphology of semiconductor nanocrystals using solution phase chemistry, which has important implications for both fundamental scientific studies and future technological application.

In our study, PbS NWs were fabricated by a hot colloidal synthesis approach [131], upon injecting trioctylphosphine sulfur into a hot reaction mixture containing lead oleate, hexadecylamine, oleic acid, and DOD-gold NPs. The NWs morphology and size were found to be dependent on the concentration of the gold particles, composition of stabilizing agents and the Pb to S molar ratio. Figures 15 and 16 show representative TEM and SEM images of NWs with a median diameter of ~35 nm and lengths up to 10 μm. The TEM and SEM images demonstrate the high degree of crystallinity and narrow diameter distribution of the NWs. To examine whether straight NWs can be produced in the absence of gold NPs, control experiments were performed at the same reaction conditions without using gold NPs. In such experiments, NWs were obtained, but these wires displayed a very different morphology with a high degree of polydispersity, irregular branched structures, and highly corrugated surfaces. The effect of gold seed particles appears to provide nucleation sites to seed one-dimensional growth of the semiconductor nanocrystals. The method demonstrated here provides a facile hot colloidal method of producing high-quality high-aspect-ratio PbS NWs of controlled diameter in high yield. In addition to NWs, other

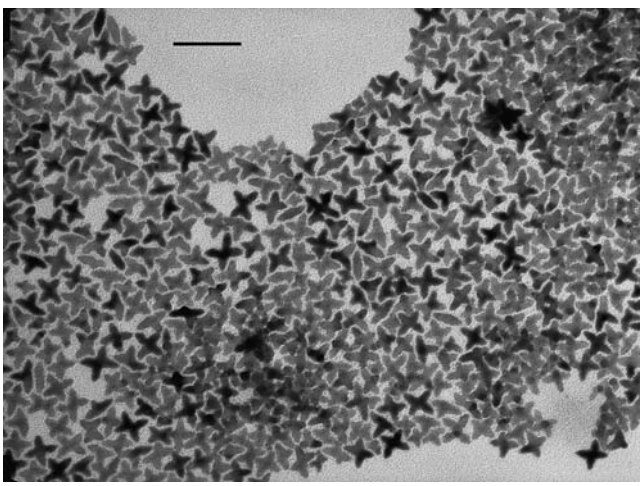

Fig. 14 TEM image of *star-shaped* PbSe NCs; the *scale bar* is 200 nm

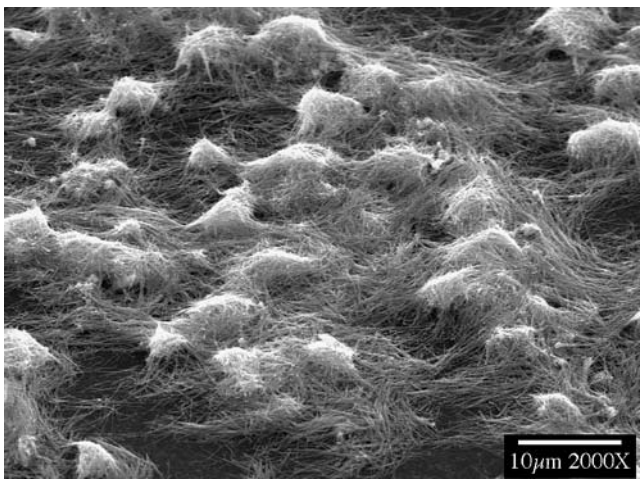

Fig. 16 SEM image of PbS NWs using gold NPs

interesting morphologies (such as gold core-PbS cube shell structures) can be obtained upon changing the concentration of gold NPs and precursor concentrations and the volume of solvent (see Figs. 17 and 18).

Comparison of anisotropic growth mechanism between the CdSe and PbSe system

Most previous studies of metal-seeded solution-phase growth of crystalline semiconductor NWs and NRs have been interpreted in terms of the SLS mechanism [86]. However, in our case, the metallic seed particles used (e.g., ~4 nm Au particles) in the experiments are too large to melt under the growth conditions (~220 °C), even accounting for size-dependent reduction of the melting point [132, 133]. In the case of CdSe, significant quantities of cadmium may dissolve in the noble metals, and this alloying would lower the melting point. This could enable a solid-state diffusion mechanism to occur in our system like that proposed for vapor–solid–solid growth of GaAs and InAs under conditions where the seed particles remain solid [107]. For the PbSe system, we also observe that the semiconductor nanocrystals cleave from the noble metal seed particles. Even though the mechanism in that case shares common features with the CdSe case, there are also notable differences. The concentration of seed particles found to be effective in seeding growth of PbSe quantum rods is roughly a factor of 100 lower than that used to seed growth of CdSe quantum rods. Also, Cd has appreciable solubility in gold; however, Pb does not; therefore, the solid-state diffusion mechanism that may be operative for CdSe probably is not possible in that case. Thus, we expect that the essential contribution of the seed particle is simply to provide a low energy interface for heterogeneous nucleation of the PbSe nanocrystal [124].

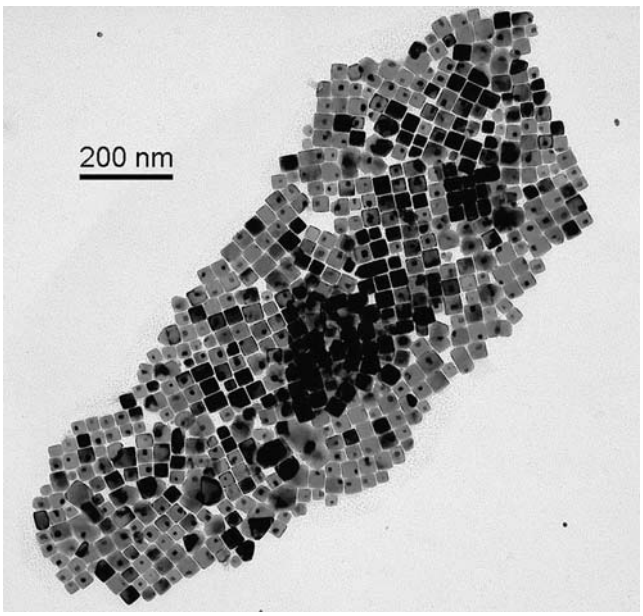

Fig. 17 TEM image of hybrid PbS-Au NPs where individual gold nanoparticle is embedded in the middle of the PbS cube particle

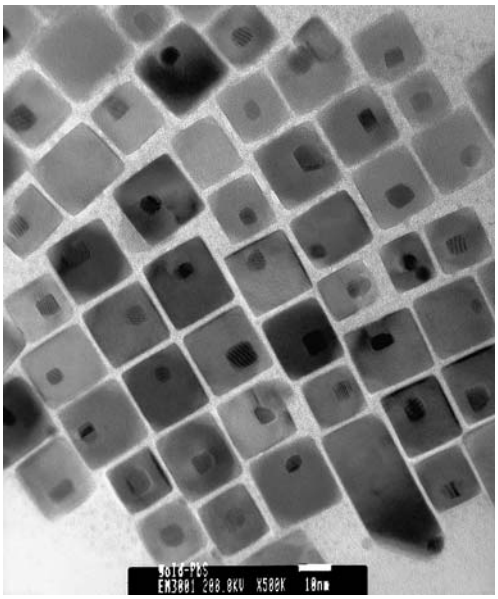

Fig. 18 HRTEM image of hybrid PbS-Au NPs where individual gold nanoparticle is embedded in the middle of the PbS cube particle

Anisotropic nanomaterials for electronic applications

It is now established that solution-processed polymeric devices with embedded semiconductor nanostructures (QDs, QRs, multipods, wires) have potential as platforms for low-cost, large-area versatile alternatives to their inorganic optoelectronic and photovoltaic counterparts [134, 135]. Semiconductor QRs or NWs, with their inherent high mobilities and large aspect ratios, are good candidates for transporting charge carriers in such hybrid devices. Recently, we have also integrated one-dimensional nano-

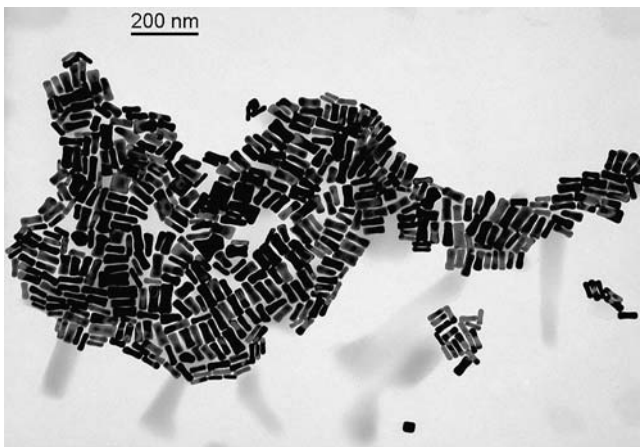

Fig. 19 TEM image of gold NRs

crystals (e.g., PbSe NRs and PbS NWs) into polymer nanocomposite photodetector devices, where they serve as an IR photosensitizer. The one-dimensional nanocrystals exhibit significant photogeneration efficiency, enabling infrared sensitization of a polymeric photoconductive nanocomposite [124, 131]. Further, careful tailoring of the nanocrystals dimensions and optimized device compositions are expected to enhance the photogeneration efficiency at the desired operating wavelength, leading to much better photoconductive performance.

Synthesis of gold NRs

The optical properties of gold NRs have recently received great attention for their applications in a variety of areas including enhanced spectroscopies, molecular electronics, gene delivery, and photothermal cancer therapy [136–138]. Gold NRs have two distinct plasmon resonance absorption bands, a longitudinal band corresponding to electron motion along the axis of the particle, and the transverse band

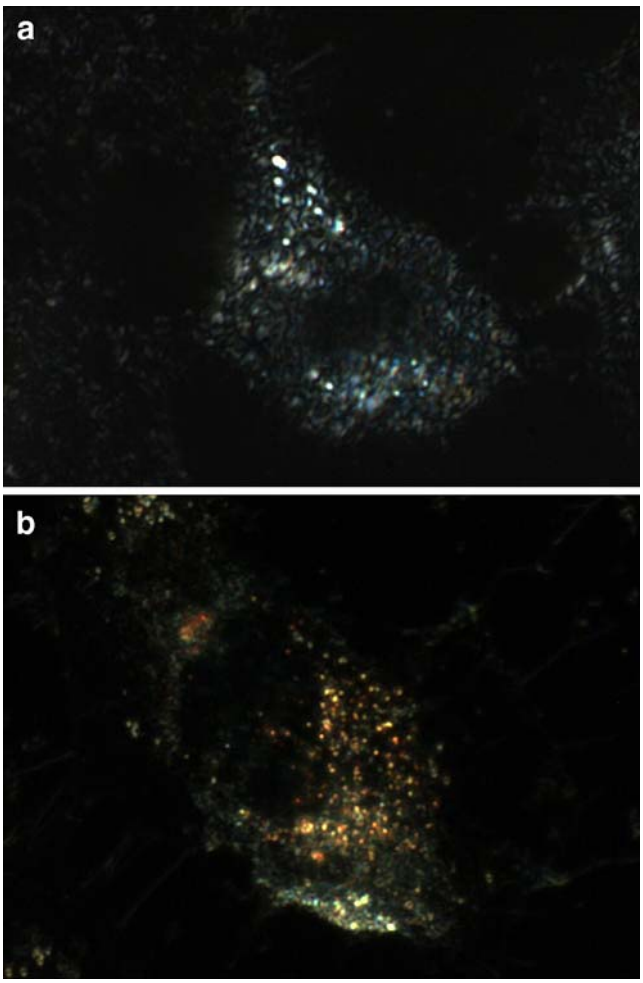

Fig. 20 Light scattering images of HeLa cells following **a** no treatment and **b** treatment with Tf-conjugated AuMLP NRs; the wavelength selective scattering (*orange*/*red*) associated with the NRs can be clearly distinguished from the background and corresponds to the surface plasmonic enhancement of the longitudinal oscillation in the red region of the optical spectra

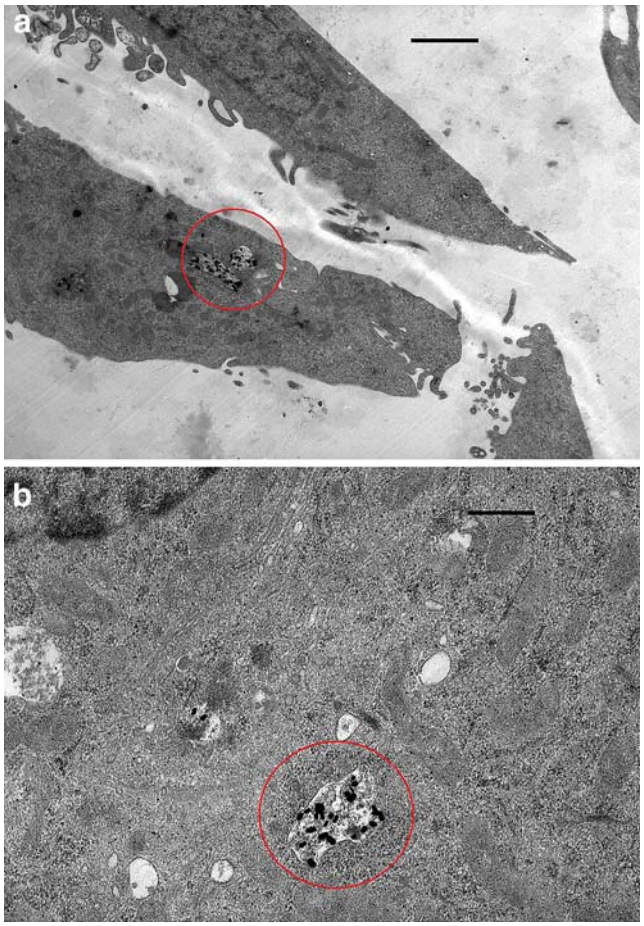

Fig. 21 TEM images **a** and **b** of HeLa cells treated with Tf-conjugated gold NRs (*circle* points out the NRs). The *scale bars* for **a** and **b** are 1,500 and 500 nm, respectively

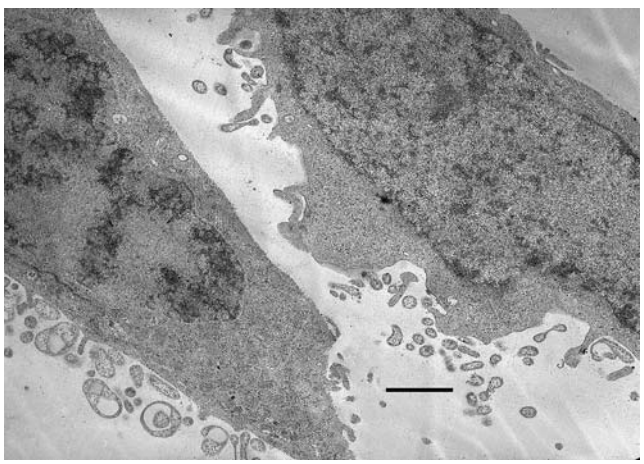

Fig. 22 TEM image of HeLa cells with unconjugated gold NRs. The *scale bar* is 1,250 nm

corresponding to motion along the short axis of the particle. Generally, the absorption maximum for the longitudinal band shifts to longer wavelengths with increasing aspect ratio. To date, many solution phase synthesis methods have been developed for preparing gold NRs. For example, the template-directed method [139], the electrochemical method [140, 141], the seed-mediated growth method [142–146], and the photochemical reduction method [147, 148] were most commonly used for fabricating gold NRs. This review only covers the seed-mediated growth method as this method has been widely used to produce monodispersed gold NRs with variable aspect ratio [149].

In our approach, CTAB was used as the primary surfactant and formed elongated micelles where the growth of rod-shaped gold NPs occurred. Silver nitrate was used promote growth of NRs rather than a mixture of various shapes of NPs (e.g., triangles and cubes) [150, 151]. Nonionic surfactants such as Tween and Triton and electrolytes such as sodium chloride and potassium chloride have been used as additives to tailor the shape, size, and aspect ratio of the gold NRs [152]. It was observed that with increasing concentrations of these additives in the growth solution, the aspect ratio of the NRs increases to a critical limit, after which it decreases again. Furthermore, upon carefully controlling the content of Triton X-100 or Tween 20 in the growth solution, these nonionic surfactants aided in fine tuning the shape of gold NRs (e.g., producing rectangular and "dogbone" shapes). Figure 19 shows a TEM image of a typical monodispered gold NR sample prepared with sodium chloride in the growth solution. The growth pattern of the NRs fits into the soft template model based on the micellar structures expected to form from the mixtures of CTAB and nonionic surfactants. More specifically, we propose that gold NRs with higher yield and aspect ratio are prone to form with more elongated CTAB micelles which provide larger surface area for gold embryo clusters [152]. This helps the gold embryo to attach longer on the micelle surface, allowing the micelle template mechanism to continue to work and prolong the growth of the gold NR.

Application of gold NRs in bioimaging

In addition to synthesizing gold NRs, we have used gold NRs coated with polyelectrolyte multilayers as biocompatible targeted optical probes for dark-field imaging as well as electron microscopy [153–157]. Transferrin (Tf)-conjugated gold NRs were used to label cancer cells. HeLa cancer cells are chosen as the target cell line. They are known to overexpress transferrin receptors. Robust receptor-mediated cellular uptake of the Tf-conjugated NRs is demonstrated from the orange/red scattering images (see Fig. 20 b), as compared to minimal uptake in the case of unconjugated NRs (see Fig. 20a). The orange/red scattering associated with the NRs originates from their strong longitudinal surface plasmon oscillation, which has a frequency in the NIR region. In addition to dark field imaging, Tf-conjugated gold NRs were also used for transmission electron microscopy. To achieve this, electron microscopy images were collected for HeLa cancer cells treated with Tf-conjugated and unconjugated NRs separately. From Fig. 21, it is evident that Tf-conjugated NRs are taken up by HeLa cells, in comparison to unconjugated NRs, which show no uptake (see Fig. 22). The endosomal localization of the NRs within the cells also suggests receptor-mediated endocytotic uptake. This is a promising demonstration of developing plasmon-enhanced scattering probes for biological applications. Most importantly, they are highly biocompatible in comparison with heavy metal-based quantum dots, especially for early in vivo cancer detection (e.g., pancreatic cancer) applications.

Summary and outlook

In summary, the solution synthetic methods developed in our group demonstrated that gold NPs can be used as a multifunctional nanoplatform to fabricate metallic nanoshells, anisotropic semiconductor nanocrystals, and gold NRs at mild conditions. The ability to easily fabricate these high quality nanomaterials in high yield will be valuable in applications such as bioimaging and bioassay technologies, light-emitting diodes, and photovoltaics. These studies provide a new direction in developing facile syntheses of different classes of NPs with unique tunable optical properties and thereby making available new building blocks for bionanotechnology.

Acknowledgements This study was supported by grants from the NCI RO1CA119397 and the John R. Oishei Foundation.

References

1. Prasad PN (2004) Nanophotonics. Wiley, New York
2. Yin Y, Alivisatos AP (2005) Nature 437:664–670 doi:10.1038/nature04165
3. Alivisatos P (2004) Nat Biotechnol 22:47–52 doi:10.1038/nbt927
4. Prasad PN (2004) Biophotonics. Wiley, New York
5. Kim S, Bawendi MG (2003) J Am Chem Soc 125:14652–14653 doi:10.1021/ja0368094
6. Zimmer JP, Kim SW, Ohnishi S, Tanaka E, Frangioni JV, Bawendi MG (2006) J Am Chem Soc 128:2526–2527 doi:10.1021/ja0579816
7. Cai W, Shin DW, Chen K, Gheysens O, Cao Q, Wang SX et al (2006) Nano Lett 6:669–676 doi:10.1021/nl052405t
8. Akerman ME, Chan WCW, Laakkonen P, Bhatia SN, Ruoslahti E (2002) Proc Natl Acad Sci U S A 99:12617–12621 doi:10.1073/pnas.152463399

9. Bruchez M Jr., Moronne M, Gin P, Weiss S, Alivisatos AP (1998) Science 281:2013–2016 doi:10.1126/science.281.5385.2013
10. Dubertret B, Skourides P, Norris DJ, Noireaux V, Brivanlou AH, Libchaber A (2002) Science 298:1759–1762 doi:10.1126/science.1077194
11. Michalet X, Pinaud FF, Bentolila LA, Tsay JM, Doose S, Li JJ et al (2005) Science 307:538–544 doi:10.1126/science.1104274
12. Chan WC, Nie S (1998) Science 281:2016–2018 doi:10.1126/science.281.5385.2016
13. Larson DR, Zipfel WR, Williams RM, Clark SW, Bruchez MP, Wise FW et al (2003) Science 300:1434–1436 doi:10.1126/science.1083780
14. Gao X, Cui Y, Levenson RM, Chung LWK, Nie S (2004) Nat Biotechnol 22:969–976 doi:10.1038/nbt994
15. Kim S, Lim YT, Soltesz EG, De Grand AM, Lee J, Nakayama A et al (2004) Nat Biotechnol 22:93–97 doi:10.1038/nbt920
16. Soo Choi H, Liu W, Misra P, Tanaka E, Zimmer JP, Itty Ipe B et al (2007) Nat Biotechnol 25:1165–1170 doi:10.1038/nbt1340
17. Bharali DJ, Lucey DW, Jayakumar H, Pudavar HE, Prasad PN (2005) J Am Chem Soc 127:1364–11371 doi:10.1021/ja051455x
18. Loo C, Lowery A, Halas N, West J, Drezek R (2005) Nano Lett 5:09–711 doi:10.1021/nl050127s
19. Levin CS, Bishnoi SW, Grady NK, Halas NJ (2006) Anal Chem 78:277–3281 doi:10.1021/ac060041z
20. Gobin AM, Lee MH, Halas NJ, James WD, Drezek RA, West JL (2007) Nano Lett 7:929–1934 doi:10.1021/nl070610y
21. Huang X, El-Sayed IH, Qian W, El-Sayed MA (2006) J Am Chem Soc 128:115–2120 doi:10.1021/ja057254a
22. El-Sayed IH, Huang X, El-Sayed MA (2005) Nano Lett 5:29–834 doi:10.1021/nl050074e
23. Peng X, Manna L, Yang W, Wickham J, Scher E, Kadavanich A et al (2000) Nature 404:59–61 doi:10.1038/35003535
24. Manna L, Milliron DJ, Meisel A, Scher EC, Alivisatos AP (2003) Nat Mater 2:82–385 doi:10.1038/nmat902
25. Burda C, Chen X, Narayanan R, El-Sayed MA (2005) Chem Rev 105:025–1102 doi:10.1021/cr030063a
26. Yong KT, Sahoo Y, Zeng H, Swihart MT, Minter JR, Prasad PN (2007) Chem Mater 19:108–4110 doi:10.1021/cm0709774
27. Mokari T, Banin U (2003) Chem Mater 15:955–3960 doi:10.1021/cm034173±
28. Panda AB, Glaspell G, El-Shall MS (2006) J Am Chem Soc 128:790–2791 doi:10.1021/ja058148b
29. Yong KT, Qian J, Roy I, Lee HH, Bergey EJ, Tramposch KM et al (2007) Nano Lett 7:61–765 doi:10.1021/nl063031m
30. Yong K-T, Roy I, Pudavar HE, Bergey EJ, Tramposch KM, Swihart MT et al (2008) Adv Mater 20:1412–1417
31. Fu A, Gu W, Boussert B, Koski K, Gerion D, Manna L et al (2007) Nano Lett 7:79–182 doi:10.1021/nl0626434
32. Li C, Curreli M, Lin H, Lei B, Ishikawa FN, Datar R et al (2005) J Am Chem Soc 127:2484–12485 doi:10.1021/ja053761g
33. Gao Z, Agarwal A, Trigg AD, Singh N, Fang C, Tung CH et al (2007) Anal Chem 79:291–3297 doi:10.1021/ac061808q
34. Shi Kam W, O'Connell M, Wisdom JA, Dai H (2005) Proc Natl Acad Sci U S A 102:1600–11605 doi:10.1073/pnas.0502680102
35. Ghosh SK, Pal T (2007) Chem Rev 107:4797–4862 doi:10.1021/cr0680282
36. Daniel MC, Astruc D (2004) Chem Rev 104:293–346 doi:10.1021/cr030698
37. Murphy CJ (2002) Science 298:2139–2141 doi:10.1126/science.1080007
38. Kelly KL, Coronado E, Zhao LL, Schatz GC (2003) J Phys Chem B 107:668–677 doi:10.1021/jp026731y
39. Yang Y, Shi J, Kawamura G, Nogami M (2008) Scr Mater 58:862–865 doi:10.1016/j.scriptamat.2008.01.017
40. Lytton-Jean AKR, Mirkin CA (2005) J Am Chem Soc 127:12754–12755 doi:10.1021/ja052255o
41. Demers LM, Ostblom M, Zhang H, Jang NH, Liedberg B, Mirkin CA (2002) J Am Chem Soc 124:11248–11249 doi:10.1021/ja0265355
42. Giljohann DA, Seferos DS, Patel PC, Millstone JE, Rosi NL, Mirkin CA (2007) Nano Lett 7:3818–3821 doi:10.1021/nl072471q
43. Storhoff JJ, Elghanian R, Mirkin CA, Letsinger RL (2002) Langmuir 18:6666–6670 doi:10.1021/la0202428
44. Nie S, Emory SR (1997) Science 275:1102–1106 doi:10.1126/science.275.5303.1102
45. Liu Y, Male KB, Bouvrette P, Luong JHT (2003) Chem Mater 15:4172–4180 doi:10.1021/cm0342041
46. Chen D-H, Chen C-J (2002) J Mater Chem 12:1557–1562 doi:10.1039/b110749f
47. Velikov KP, Zegers GE, van Blaaderen A (2003) Langmuir 19:1384–1389 doi:10.1021/la026610p
48. Pastoriza-Santos I, Liz-Marzan LM (2002) Langmuir 18:2888–2894 doi:10.1021/la015578g
49. Zhao X, Mai Z, Kang X, Dai Z, Zou X (2008) Electrochim Acta 53:4732–4739 doi:10.1016/j.electacta.2008.02.007
50. Ma Z, Han H (2008) Colloids Surf A Physicochem Eng Asp 317:229–233 doi:10.1016/j.colsurfa.2007.10.018
51. Wang W, Chen X, Efrima S (1999) J Phys Chem B 103:7238–7246 doi:10.1021/jp991101q
52. Jiang X, Xie Y, Lu J, Zhu L, He W, Qian Y (2001) Langmuir 17:3795–3799 doi:10.1021/la001361v
53. Neiman B, Grushka E, Lev O (2001) Anal Chem 73:5220–5227 doi:10.1021/ac0104375
54. Zhu J, Liu S, Palchik O, Koltypin Y, Gedanken A (2000) Langmuir 16:6396–6399 doi:10.1021/la991507u
55. Pastoriza-Santos I, Liz-Marzan LM (1999) Langmuir 15:948–951 doi:10.1021/la980984u
56. Tan Y, Jiang L, Li Y, Zhu DJ (2002) Phys Chem B 106:3131–3138 doi:10.1021/jp012668l
57. Manna A, Imae T, Aoi K, Okada M, Yogo T (2001) Chem Mater 13:1674–1681 doi:10.1021/cm000416b
58. Hall SR, Davis SA, Mann S (2000) Langmuir 16:1454–1456 doi:10.1021/la9909143
59. Pham T, Jackson JB, Halas NJ, Lee TR (2002) Langmuir 18:4915–4920 doi:10.1021/la015561y
60. Nikoobakht B, El-Sayed MA (2003) Chem Mater 15:1957–1962 doi:10.1021/cm020732l
61. Nikoobakht B, El-Sayed MA (2001) Langmuir 17:6368–6374 doi:10.1021/la010530o
62. Leff DV, Brandt L, Heath JR (1996) Langmuir 12:4723–4730 doi:10.1021/la960445u
63. Nehl CL, Grady NK, Goodrich GP, Tam F, Halas NJ, Hafner JH (2004) Nano Lett 4:2355–2359 doi:10.1021/nl048610a
64. Choi MR, Stanton-Maxey KJ, Stanley JK, Levin CS, Bardhan R, Akin D et al (2007) Nano Lett 7:3759–3765 doi:10.1021/nl072209h
65. Yong K-T, Sahoo Y, Swihart MT, Prasad PN (2006) Colloids Surf A Physicochem Eng Asp 290:89–105 doi:10.1016/j.colsurfa. 2006.05.004
66. Shi W, Sahoo Y, Swihart MT, Prasad PN (2005) Langmuir 21:1610–1617 doi:10.1021/la047628y
67. Gerion D, Chen F, Kannan B, Fu A, Parak WJ, Chen DJ et al (2003) Anal Chem 75:4766–4772 doi:10.1021/ac034482j
68. Talapin DV, Koeppe R, Gotzinger S, Kornowski A, Lupton JM, Rogach AL et al (2003) Nano Lett 3:1677–1681 doi:10.1021/nl034815s
69. Talapin DV, Mekis I, Gotzinger S, Kornowski A, Benson O, Weller H (2004) J Phys Chem B 108:18826–18831 doi:10.1021/jp046481g
70. Murray CB, Kagan CR, Bawendi MG (1995) Science 270:1335–1338 doi:10.1126/science.270.5240.1335

71. Gerion D, Pinaud F, Williams SC, Parak WJ, Zanchet D, Weiss S et al (2001) J Phys Chem B 105:8861–8871 doi:10.1021/jp0105488
72. Fu A, Micheel CM, Cha J, Chang H, Yang H, Alivisatos AP (2004) J Am Chem Soc 126:10832–10833 doi:10.1021/ja046747x
73. Qian J, Yong KT, Roy I, Ohulchanskyy TY, Bergey EJ, Lee HH et al (2007) J Phys Chem B 111:6969–6972 doi:10.1021/jp070620n
74. Jiang XC, Xiong QH, Nam S, Qian F, Li Y, Lieber CM (2007) Nano Lett 7:3214–3218 doi:10.1021/nl072024a
75. Javey A, Nam S, Friedman RS, Yan H, Lieber CM (2007) Nano Lett 7:773–777 doi:10.1021/nl063056l
76. Barrelet CJ, Bao JM, Loncar M, Park HG, Capasso F, Lieber CM (2006) Nano Lett 6:11–15 doi:10.1021/nl0522983
77. Agarwal R, Barrelet CJ, Lieber CM (2005) Nano Lett 5:917–920 doi:10.1021/nl050440u
78. Qian F, Li Y, Gradecak S, Wang DL, Barrelet CJ, Lieber CM (2004) Nano Lett 4:1975–1979 doi:10.1021/nl0487774
79. Liu J, Fei P, Zhou J, Tummala R, Wang ZL (2008) Appl Phys Lett 92:173105
80. Qin Y, Wang XD, Wang ZL (2008) Nature 451:809–U5 doi:10.1038/nature06601
81. Lin YF, Song J, Ding Y, Lu SY, Wang ZL (2008) Appl Phys Lett 92:022105
82. Wang XD, Liu J, Song JH, Wang ZL (2007) Nano Lett 7:2475–2479 doi:10.1021/nl0712567
83. Zou BS, Liu RB, Wang FF, Pan AL, Cao L, Wang ZL (2006) J Phys Chem B 110:12865–12873 doi:10.1021/jp061357d
84. Kim W, Ng JK, Kunitake ME, Conklin BR, Yang P (2007) J Am Chem Soc 129:7228–7229 doi:10.1021/ja071456k
85. Morales AM, Lieber CM (1998) Science 279:208–211 doi:10.1126/science.279.5348.208
86. Trentler TJ, Hickman KM, Goel SC, Viano AM, Gibbons PC, Buhro WE (1995) Science 270:1791–1794 doi:10.1126/science.270.5243.1791
87. Peng ZA, Peng X (2001) J Am Chem Soc 123:183–184 doi:10.1021/ja003633m
88. Xie R, Battaglia D, Peng X (2007) J Am Chem Soc 129:15432–15433 doi:10.1021/ja076363h
89. Peng ZA, Peng X (2002) J Am Chem Soc 124:3343–3353 doi:10.1021/ja0173167
90. Peng ZA, Peng X (2001) J Am Chem Soc 123:1389–1395 doi:10.1021/ja0027766
91. Stach EA, Pauzauskie PJ, Kuykendall T, Goldberger J, He R, Yang P (2003) Nano Lett 3:867–869 doi:10.1021/nl034222h
92. Ding Y, Gao PX, Wang ZL (2004) J Am Chem Soc 126:2066–2072 doi:10.1021/ja039354r
93. Bakkers EPAM, Verheijen MA (2003) J Am Chem Soc 125:3440–3441 doi:10.1021/ja0299102
94. Kuno M, Ahmad O, Protasenko V, Bacinello D, Kosel TH (2006) Chem Mater 18:5722–5732 doi:10.1021/cm061559m
95. Hull KL, Grebinski JW, Kosel TH, Kuno M (2005) Chem Mater 17:4416–4425 doi:10.1021/cm050952±
96. Danek M, Jensen KF, Murray CB, Bawendi MG (1996) Chem Mater 8:173–180 doi:10.1021/cm9503137
97. Protasenko V, Bacinello D, Kuno M (2006) J Phys Chem B 110:25322–25331 doi:10.1021/jp066034w
98. Robel I, Bunker BA, Kamat PV, Kuno M (2006) Nano Lett 6:1344–1349 doi:10.1021/nl060199z
99. Ma C, Wang ZL (2005) Adv Mater 17:2635–2639 doi:10.1002/adma.200500805
100. Xi LF, Lam YM, Xu YP, Li LJ (2008) J Colloid Interface Sci 320:491–500 doi:10.1016/j.jcis.2008.01.048
101. Panda AB, Glaspell G, El-Shall MS (2008) J Am Chem Soc 130:4203–4203 doi:10.1021/ja8003717
102. Puthussery J, Lan A, Kosel TH, Kuno M (2008) ACS Nano 2:357–367 doi:10.1021/nn700270a
103. Lu X, Hanrath T, Johnston KP, Korgel BA (2003) Nano Lett 3:93–99 doi:10.1021/nl0202307
104. Hanrath T, Korgel BA (2002) J Am Chem Soc 124:1424–1429 doi:10.1021/ja016788i
105. Schricker AD, Joshi SV, Hanrath T, Banerjee SK, Korgel BA (2006) J Phys Chem B 110:6816–6823 doi:10.1021/jp055663n
106. Yu H, Li J, Loomis RA, Gibbons PC, Wang LW, Buhro WE (2003) J Am Chem Soc 125:16168–16169 doi:10.1021/ja037971
107. Yong K-T, Sahoo Y, Swihart MT, Prasad PN (2006) Adv Mater 18:1978–1982 doi:10.1002/adma.200600368
108. Acharya S, Patla I, Kost J, Efrima S Golan Y (2006) J Am Chem Soc 128:9294–9295 doi:10.1021/ja062404i
109. Dong L, Gushtyuk T, Jiao J (2004) J Phys Chem B 108:1617–1620 doi:10.1021/jp0364811
110. Sun SQ, Li T (2007) Cryst Growth Des 7:2367–2371 doi:10.1021/cg060529t
111. Zhang P, Gao L (2003) Langmuir 19:208–210 doi:10.1021/la0206458
112. Barrelet CJ, Wu Y, Bell DC, Lieber CM (2003) J Am Chem Soc 125:11498–11499 doi:10.1021/ja036990g
113. Datta A, Panda SK, Chaudhuri S (2007) J Phys Chem C 111:17260–17264 doi:10.1021/jp076093p
114. Saunders AE, Popov I, Banin U (2006) J Phys Chem B 110:25421–25429 doi:10.1021/jp065594s
115. Jang JS, Joshi UA, Lee JS (2007) J Phys Chem C 111:13280–13287 doi:10.1021/jp072683b
116. Yong KT, Sahoo Y, Swihart MT, Prasad PN (2007) J Phys Chem C 111:2447–2458 doi:10.1021/jp066392z
117. Wang X, Xi G, Liu Y, Qian Y (2008) Cryst Growth Des 8:1406–1411 doi:10.1021/cg070415x
118. Pietryga JM, Schaller RD, Werder D, Stewart MH, Klimov VI, Hollingsworth JA (2004) J Am Chem Soc 126:11752–11753 doi:10.1021/ja047659f
119. Houtepen AJ, Koole R, Vanmaekelbergh D, Meeldijk J, Hickey SG (2006) J Am Chem Soc 128:6792–6793 doi:10.1021/ja061644v
120. Cao H, Gong Q, Qian X, Wang H, Zai J, Zhu Z (2007) Cryst Growth Des 7:425–429 doi:10.1021/cg060415h
121. Zhu J, Aruna ST, Koltypin Y, Gedanken A (2000) Chem Mater 12:143–147 doi:10.1021/cm990459w
122. Lu W, Gao P, Jian WB, Wang ZL, Fang J (2004) J Am Chem Soc 126:14816–14821 doi:10.1021/ja046769j
123. Choudhury KR, Sahoo Y, Prasad PN (2005) Adv Mater 17:2877–2881 doi:10.1002/adma.200501489
124. Yong KT, Sahoo Y, Choudhury KR, Swihart MT, Minter JR, Prasad PN (2006) Nano Lett 6:709–714 doi:10.1021/nl052472n
125. Ni Y, Liu H, Wang F, Liang Y, Hong J, Ma X et al (2004) Cryst Growth Des 4:759–764 doi:10.1021/cg034103f
126. Ma Y, Qi L, Ma J, Cheng H (2004) Cryst Growth Des 4:351–354 doi:10.1021/cg034174e
127. Bierman MJ, Lau YKA, Jin S (2007) Nano Lett 7:2907–2912 doi:10.1021/nl071405l
128. Lee SM, Jun YW, Cho SN, Cheon J (2002) J Am Chem Soc 124:11244–11245 doi:10.1021/ja026805j
129. Gao F, Lu Q, Liu X, Yan Y, Zhao D (2001) Nano Lett 1:743–748 doi:10.1021/nl0156383
130. Chen J, Chen L, Wu LM (2007) Inorg Chem 46:8038–8043 doi:10.1021/ic7008336
131. Yong KT, Sahoo Y, Choudhury KR, Swihart MT, Minter JR, Prasad PN (2006) Chem Mater 18:5965–5972 doi:10.1021/cm061771q
132. Tuan HY, Lee DC, Hanrath T, Korgel BA (2005) Chem Mater 17:5705–5711 doi:10.1021/cm0513031

133. Tuan HY, Lee DC, Hanrath T, Korgel BA (2005) Nano Lett 5:681–684 doi:10.1021/nl050099d
134. Huynh WU, Dittmer JJ, Alivisatos AP (2002) Science 295:2425–2427 doi:10.1126/science.1069156
135. Gur I, Fromer NA, Geier ML, Alivisatos AP (2005) Science 310:462–465 doi:10.1126/science.1117908
136. Caswell KK, Wilson JN, Bunz UHF, Murphy CJ (2003) J Am Chem Soc 125:13914–13915 doi:10.1021/ja037969i
137. Stone JW, Sisco PN, Goldsmith EC, Baxter SC, Murphy C (2007) J Nano Lett 7:116–119 doi:10.1021/nl062248d
138. Wu HY, Huang WL, Huang MH (2007) Cryst Growth Des 7:831–835 doi:10.1021/cg060788i
139. Moon JM, Wei A (2005) J Phys Chem B 109:23336–23341 doi:10.1021/jp054405n
140. Yu YY, Chang SS, Lee CL, Wang CRC (1997) J Phys Chem B 101:6661–6664 doi:10.1021/jp971656q
141. Tian Y, Liu H, Zhao G, Tatsuma T (2006) J Phys Chem B 110:23478–23481 doi:10.1021/jp065292q
142. Sau TK, Murphy CJ (2004) J Am Chem Soc 126:8648–8649 doi:10.1021/ja047846d
143. Jana NR, Gearheart L, Murphy CJ (2001) J Phys Chem B 105:4065–4067 doi:10.1021/jp0107964
144. Gou L, Murphy C (2005) Chem Mater 17:3668–3672 doi:10.1021/cm050525w
145. Gao J, Bender CM, Murphy CJ (2003) Langmuir 19:9065–9070 doi:10.1021/la034919i
146. Wu HY, Chu HC, Kuo TJ, Kuo CL, Huang MH (2005) Chem Mater 17:6447–6451 doi:10.1021/cm051455w
147. Kim F, Song JH, Yang P (2002) J Am Chem Soc 124:14316–14317 doi:10.1021/ja028110o
148. Nishioka K, Niidome Y, Yamada S (2007) Langmuir 23:10353–10356 doi:10.1021/la7015534
149. Gole A, Murphy CJ (2004) Chem Mater 16:3633–3640 doi:10.1021/cm0492336
150. Zijlstra P, Bullen C, Chon JWM, Gu M (2006) J Phys Chem B 110:19315–19318 doi:10.1021/jp0635866
151. Chen HM, Peng HC, Liu RS, Asakura K, Lee CL, Lee JF et al (2005) J Phys Chem B 109:19553–19555 doi:10.1021/jp053657l
152. Yong K-T, Sahoo Y, Swihart M, Schneeberger P, Prasad P (2008) Top Catal 47:49–60 doi:10.1007/s11244-007-9030-7
153. Gole A, Murphy CJ (2005) Chem Mater 17:1325–1330 doi:10.1021/cm048297d
154. Oyelere AK, Chen PC, Huang X, El-Sayed IH, El-Sayed MA (2007) Bioconjug Chem 18:1490–1497 doi:10.1021/bc070132i
155. Ding H, Yong KT, Roy I, Pudavar HE, Law WC, Bergey EJ et al (2007) J Phys Chem C 111:12552–12557 doi:10.1021/jp0733419
156. Liao H, Hafner JH (2005) Chem Mater 17:4636–4641 doi:10.1021/cm050935k
157. Yu C, Nakshatri H, Irudayaraj J (2007) Nano Lett 7:2300–2306 doi:10.1021/nl070894m